Six-Month Outcomes of Clinically Relevant Meniscal Injury in a Large-Animal Model

Sonia Bansal,*†‡ PhD, Kyle D. Meadows,§ BSE, Liane M. Miller,*† MD, Kamiel S. Saleh,*† BS, Jay M. Patel,*† PhD, Brendan D. Stoeckl,*† MSE, Elisabeth A. Lemmon,*† BS, Michael W. Hast,*†‖ PhD, Miltiadis H. Zgonis,*† MD, Carla R. Scanzello,†¶ MD, PhD, Dawn M. Elliott,§ PhD, and Robert L. Mauck,*†‡# PhD
Investigation performed at University of Pennsylvania, Philadelphia, Pennsylvania, USA

Background: The corrective procedures for meniscal injury are dependent on tear type, severity, and location. Vertical longitudinal tears are common in young and active individuals, but their natural progression and impact on osteoarthritis (OA) development are not known. Root tears are challenging and they often indicate poor outcomes, although the timing and mechanisms of initiation of joint dysfunction are poorly understood, particularly in large-animal and human models.

Purpose/Hypothesis: In this study, vertical longitudinal and root tears were made in a large-animal model to determine the progression of joint-wide dysfunction. We hypothesized that OA onset and progression would depend on the extent of injury-based load disruption in the tissue, such that root tears would cause earlier and more severe changes to the joint.

Study Design: Controlled laboratory study.

Methods: Sham surgeries and procedures to create either vertical longitudinal or root tears were performed in juvenile Yucatan mini pigs through randomized and bilateral arthroscopic procedures. Animals were sacrificed at 1, 3, or 6 months after injury and assessed at the joint and tissue level for evidence of OA. Functional measures of joint load transfer, cartilage indentation mechanics, and meniscal tensile properties were performed, as well as histological evaluation of the cartilage, meniscus, and synovium.

Results: Outcomes suggested a progressive and sustained degeneration of the knee joint and meniscus after root tear, as evidenced by histological analysis of the cartilage and meniscus. This occurred in spite of spontaneous reattachment of the root, suggesting that this reattachment did not fully restore the function of the native attachment. In contrast, the vertical longitudinal tear did not cause significant changes to the joint, with only mild differences compared with sham surgery at the 6-month time point.

Conclusion: Given that the root tear, which severs circumferential connectivity and load transfer, caused more intense OA compared with the circumferentially stable vertical longitudinal tear, our findings suggest that without timely and mechanically competent fixation, root tears may cause irreversible joint damage.

Clinical Relevance: More generally, this new model can serve as a test bed for experimental surgical, scaffold-based, and small molecule–driven interventions after injury to prevent OA progression.

Keywords: knee; meniscus; biomechanics; general; medical aspects of sports; microscopic pathology

Given the primary load-bearing role of the knee meniscus, injury is common, with an incidence of 66 per 100,000 persons each year.[51] These injuries result in physical disruption of the tissue, in the form of tears that are diverse in type, severity, size, orientation, and location.[19,51] Tears may be acute (and concomitant with another traumatic event in the joint), or they may be degenerative (occurring in a low-energy setting) and arise from a loss of tissue structure/function. With time, these injuries are highly likely to be correlated with osteoarthritis (OA).[66] The International

Society of Arthroscopy, Knee Surgery and Orthopaedic Sports Medicine (ISAKOS) developed a classification system to describe tear characteristics and type,[15,17] with the classification of tear type directing their clinical management. While any injury to the meniscus is likely to instigate inflammation, tears that compromise mechanical function typically produce a sustained cascade of degeneration in the knee. For example, while incomplete (<90% width) radial longitudinal tears show maintenance of load transfer,[9,50] large horizontal tears result in increased tibial contact pressure compared with uninjured controls.[8] Even tears that are small in size initially may propagate with time, resulting in larger and more complex tears or complete maceration of the tissue, with subsequent pain and dysfunction.

One of the most common tears in young, active individuals is the vertical longitudinal tear.[17] These tears traverse along circumferential fibers and transect the orthogonal radial fiber network, which acts to resist radial expansion and longitudinal splitting.[17] They are most commonly traumatic,[35] nondegenerative, and are also considered to be the best-case scenario for meniscal repair.[80] For smaller, stable tears (<10-mm length) in the avascular zone, the normal clinical strategy is no treatment.[80] When they are larger and in the red or red-white vascularized zone,[3] vertical longitudinal tears can be suture repaired using outside-in, inside-out, or all-inside techniques. These are usually addressed soon after diagnosis, given that they have the potential to extend into a more problematic displaced bucket-handle tear.[80] While vertical longitudinal tears have better clinical outcomes than other tear types, they can cause mechanical perturbations to the joint, especially when large in size. In terms of peak contact pressure on the tibial plateau, small (<1.5 cm) vertical longitudinal tears in the posterior horn cause no change,[27] whereas larger (2.5 cm) vertical longitudinal tears increase peak contact pressure compared with intact controls.[13] Similarly, large vertical longitudinal tears in the body of the meniscus result in decreased strain in the anterior horn compared with intact controls.[31] Thus, if left untreated or if healing is insufficient, large vertical longitudinal tears may affect load transfer, become larger, or both. Given their commonality, there is a need for further investigation of the natural progression of this tear type under controlled conditions.

While vertical longitudinal tears may progress in size, resulting in abnormal joint stress distribution, other tear types result in an immediate change in knee mechanics. For example, complete root tears sever the meniscotibial attachment and are most commonly observed at the posterior attachment. These tears are challenging to treat, easy to miss, and without appropriate fixation, cause altered joint loading[56] and significant risk of cartilage degeneration, subchondral fracture, and progressive OA.[11] After vertical longitudinal tear, suture repair is advised if possible,[10,17,32,35,36,42,80] given that absent repair, patients invariably have poor outcomes.[37] This is thought to be because root tears lead to marked changes in the load-bearing function of the meniscus. With a root tear, the medial meniscus is susceptible to extrusion.[34] The loss of hoop stress and increased meniscal extrusion after a root tear results in reduced contact area between the meniscus and tibia, and increased peak loads on the tibial plateau cartilage,[56,84] which then leads to rapid cartilage degeneration.[17,80] In small- and large-animal models, a surgical destabilization of the medial meniscus (DMM)—the equivalent of a root tear—has been effectively used to instigate joint degeneration by a number of research groups.** Specifically, anterior release was performed by Oláh and colleagues[55] in a sheep model and by Waller and colleagues[81] in a porcine model. In addition, multiple papers by the Cook group[39,46,57] describe a canine arthroscopic posterior meniscal release model and associated outcomes. Given the severity of joint degeneration subsequent to root tears, there is also need for further investigation of the natural progression of this tear type under controlled conditions.

Although it is clear that adverse outcomes arise after meniscal tears, additional work is needed to define the trajectory of joint disease after these injuries. Human clinical studies provide insight into postoperative outcomes and long-term follow-up, but they generally rely on patient-reported outcomes and do not provide high spatiotemporal resolution in terms of changes in cartilage and meniscus after injury.[11,37,73] Small-animal models, on the other hand, have been used extensively to investigate cartilage and joint changes after injury, but these changes typically occur over accelerated time intervals relative to humans, and the small animal size does not provide for assessment of the meniscus itself.[14,18,26,28,45,49] Additionally, these studies largely utilize the DMM surgical technique and do not address other clinically relevant meniscal injuries. To that end, we and others look to large-animal models to fill this knowledge gap in the field of meniscal injury and to investigate cartilage and joint pathology over time scales relevant to the human disease.[46,55,81]

**References 6, 14, 18, 26, 28, 39, 45, 46, 49, 54, 55, 57, 81.

#Address correspondence to Robert L. Mauck, PhD, Department of Orthopedic Surgery, University of Pennsylvania, 3450 Hamilton Walk, 371 Stemmler Hall, Philadelphia, PA 19104, USA (email: lemauck@pennmedicine.upenn.edu) (Twitter: @MauckLab).

*McKay Orthopaedic Research Laboratory, Department of Orthopaedic Surgery, Perelman School of Medicine, University of Pennsylvania, Philadelphia, Pennsylvania, USA.

†Translational Musculoskeletal Research Center, Corporal Michael J. Crescenz VA Medical Center, Philadelphia, Pennsylvania, USA.

‡Department of Bioengineering, University of Pennsylvania, Philadelphia, Pennsylvania, USA.

§Department of Biomedical Engineering, University of Delaware, Newark, Delaware, USA.

∥Biedermann Lab for Orthopaedic Research, Department of Orthopaedic Surgery, Perelman School of Medicine, University of Pennsylvania, Philadelphia, Pennsylvania, USA.

¶Division of Rheumatology, University of Pennsylvania, Philadelphia, Pennsylvania, USA.
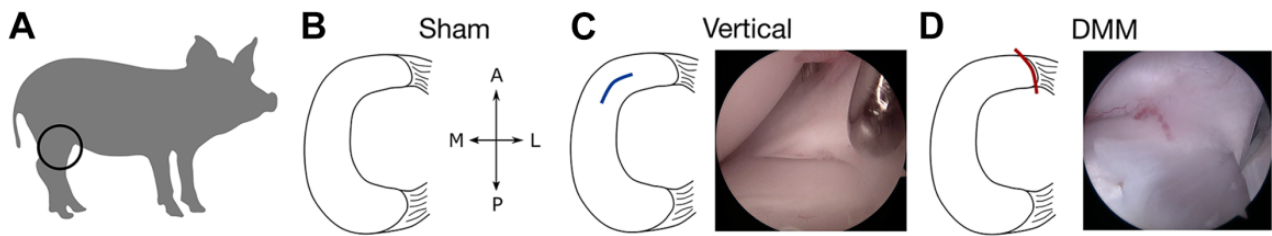
Figure 1. Schematic of experimental groups. (A) Yucatan minipigs (juvenile; age 6 months) were subjected to (B) sham surgery (arthroscopic meniscal visualization), (C) introduction of an acute arthroscopic vertical defect in the anterior horn, or (D) destabilization of the medial meniscus (DMM) via acute arthroscopic transection of the anterior horn attachment. A, anterior; L, lateral; M, medial; P, posterior.

TABLE 1
Sample Sizes per Experimental Treatment Group
at Each Time Point[a]

	1 mo	3 mo	6 mo
Sham	5[b]	6[b]	5
Vertical	6	7	4
DMM	6[b]	7[b]	5

[a]DMM, destabilization of the medial meniscus.
[b]Data previously published in part (Bansal et al[6]).

The goal of this study was to determine the spatiotemporal progression of joint pathology after surgically induced vertical longitudinal tear or root tear (via DMM) in a large-animal model. To accomplish this goal, we developed an arthroscopic meniscal injury model in the Yucatan minipig and evaluated outcomes at 1, 3, and 6 months after injury. Here we report the longer term time points, additional assays, and comparison between DMM and vertical longitudinal injury, with a focus on 6-month results. We hypothesized that DMM would cause joint degeneration at earlier time points, whereas vertical longitudinal tears would take longer to show degeneration.

METHODS

Study Design

This study received ethics approval from the Institutional Animal Care and Use Committee of the University of Pennsylvania. A total of 51 stifle joints (Figure 1A) in 32 Yucatan minipigs (Sinclair Bioresources, average age: 7.4 ± 1.2 months [range, 6.1-10.2 months]; castrated males, average weight: 28.6 ± 4.2 kg [range, 19-35 kg]; bilateral surgeries) underwent arthroscopic surgery between February 15, 2018, and June 20, 2019. Animals were euthanized at 1, 3, or 6 months after surgery. Experimental conditions included an arthroscopic sham control (sham group; n = 5 at 1 month, n = 6 at 3 months, n = 5 at 6 months), a vertical longitudinal defect approximately 4 to 5 mm (vertical group; n = 6 at 1 month, n = 7 at 3 months, n = 4 at 6 months), and DMM[26] (DMM group; n = 6 at 1 month, n = 7 at 3 months, n = 5 at 6 months) and were randomized

across stifle joints (Table 1). Data from a subset (sham and DMM, 1- and 3-month time points) of these animals have been previously reported[6] and were used to establish the model system.

Animal Model and Surgical Procedures

Arthroscopic sham and DMM surgeries were performed as reported previously.[6] Briefly, a No. 11 scalpel blade was used to create lateral and medial parapatellar vertical 2-cm skin incisions, and sterile lactated Ringer solution was used to insufflate the joint. The meniscus was visualized after trimming of the fat pad using an arthroscopic shaver (Stryker). Sham surgeries consisted of verification that the medial meniscus was attached to the tibial plateau using a right-angle probe (Figure 1B). Vertical longitudinal tears (approximately 4-5 mm) were created in the red-white zone of the medial meniscus at the junction of the anterior horn and body using either a No. 11 scalpel blade or an 18-gauge needle (Figure 1C and Supplemental Video 1). To ensure that a full-thickness defect was created, a right-angled probe was placed into the defect and advanced through to the articular cartilage. DMM was performed via a complete transection of the anterior horn of the medical meniscus[26] with a No. 11 scalpel blade[6] (Figure 1D and Supplemental Video 2). To confirm DMM, a probe was used to confirm that the attachment was fully detached.

Magnetic Resonance Imaging

After the animals were euthanized, the intact hindlimbs were removed, skin and excess musculature of the thigh were dissected away, and samples were hydrated in pads soaked with phosphate-buffered saline (PBS). Magnetic resonance imaging (MRI) scanning was carried out as previously described[6] using high-resolution T_1 volumetric interpolated breath-hold examination (VIBE) and multislice-multiecho (MSME) T_2-weighted mapping sequences,[52] with a 30- to 35-minute total scan time. T_2 relaxation time was quantified in the anterior and posterior horns of the medial meniscus and the cartilage-cartilage and cartilage-meniscus contact areas of the medial tibial plateau, as described previously.[6] We chose these T_1 VIBE and T_2 mapping sequences to quantify geometry and relaxation times, respectively, as these sequences are available

on our MRI scanner, yet other sequences such as FLASH (Fast Low-angle Shot), $T_{1\rho}$, or UTE (Ultrashort echo time) would also be appropriate to obtain these quantitative measures.[53,64,71,76] After completing all scans, samples were frozen at $-20°$C.

Measurement of Load Transfer in the Stifle

Stifles were thawed overnight and dissected as described previously, keeping ligaments intact.[6] Joints were fixed at 45° of flexion[25,63,75] in a custom aluminum testing jig. Thin-film pressure sensors (I-Scan 6900; TekScan) were equilibrated and calibrated no more than 24 hours before testing,[82] before being sealed with waterproof tape to create an extended tab for insertion. The joint capsule was dissected anteriorly and posteriorly to allow for sensors to be inserted between the meniscus and the tibial plateau. A universal joint was used in line with the jig, allowing for the tibia to move in varus/valgus. This ensured tibiofemoral contact in both compartments of the knee throughout testing. A universal test frame (ElectroForce 3550; TA Instruments) was used to apply dynamic load to the overall joint (10-400 N, 100 cycles, 1 Hz, sinusoidal). Upon the completion of testing, contact areas and peak contact pressures were analyzed when a total of 100 N was measured on the medial compartment.[70]

Macroscopic Assessment of the Joint

Immediately after pressure distribution analysis, synovium was collected from the suprapatellar space and frozen at $-20°$C. Joints were then dissected further by severing the collateral ligaments, and medial and lateral menisci were removed from the tibial plateau. After gross imaging, both medial and lateral menisci (including the anterior attachments) were wrapped in PBS-soaked gauze and frozen at $-20°$C. Additional gross images were taken of the cartilaginous surfaces with and without India ink staining,[16,21,46,60,81] and staining patterns were categorized as "no wear," "minor wear" (surface roughening in less than one-fourth of the total area of any one condyle or plateau), or "major wear" (cartilage lesion and/or surface roughening in more than one-fourth of any one condyle or plateau).

Measurement of Cartilage Mechanical Properties

Osteochondral segments (medial-lateral span of the tibial plateau × 20 mm in the anterior-posterior direction) were taken from the medial tibial plateaus of each joint and potted in poly(methyl-methacrylate) (Ortho Jet; Lang Dental Manufacturing) and were oriented orthogonally to an impermeable, stainless steel spherical indenter (Ø = 2 mm). Samples were hydrated with PBS with protease inhibitors (Sigma-Aldrich) to prevent degradation during indentation testing.[47] In both the cartilage-cartilage (area not covered by the meniscus) and the cartilage-meniscus contact area, 4 consecutive stress-relaxation steps (each 0.065-mm displacement at 0.00065 mm/s) were performed, with 600 seconds of relaxation between each step. The thickness of each sample was determined from micro–computed tomography (microCT) images (see the next section),

and this value was used to calculate the applied strain and equilibrium modulus at the second strain step.

MicroCT of Osteochondral Segments

After indentation testing, osteochondral samples were fixed in 10% neutral buffered formalin (NBF; Sigma-Aldrich) for at least 24 hours and subsequently scanned in a microCT50 (Scanco) at 70 kV and 85 µA. Subchondral bone volume per total volume (BV/TV) and trabecular thickness was calculated. As described previously,[6] superficial (cartilage-bone interface to 1 mm deep) and deep (2-5 mm deep) cylindrical volumes of interest (Ø = 5 mm) were analyzed in both the cartilage-cartilage and the cartilage-meniscus contact areas.[21,22,60]

Cartilage Histology

After microCT analysis, samples were decalcified (Formical-2000; Thermo Fisher Scientific) for a minimum of 14 days and subsequently paraffin processed and embedded. Then, 8 µm–thick sections were cut and stained with safranin-O/fast green to visualize proteoglycan content of the matrix. Three blinded reviewers (S.B., K.S.S., J.M.P.) scored the histological images using the Osteoarthritis Research Society International (OARSI) histopathology guidelines for sheep and goats, which specifically looks at subcategories of cartilage structure, cell number, cell cloning, proteoglycan staining, and tidemark integrity.[44] Sections from each time point were stained, imaged at 20× magnification (Aperio; Leica Biosystems), and scored independently. The median score of the 3 reviewers in each subcategory was summed to yield the final score for each sample.

Meniscal Sectioning and Sample Preparation

Medial menisci were prepared for further analysis as in previous work.[7] Briefly, anterior and posterior horns were separated from the meniscal body. These were radially sectioned to yield a wedge-shaped cross section using a cryostat (model HM500; Microm International GmbH). From the body-horn junction, 16 µm–thick radial sections were cut (n = 20-25 sections/horn). Attachment regions were similarly sectioned to a 16-µm thickness (n = 8-12 sections/attachment) in the radial direction. The 16 µm–thick sections were used for histological analysis. The remaining meniscal body segments were sectioned in the transverse plane. After removal of the top one-third of the tissue, 16 µm–thick sections (n = 3-4 sections/meniscus) were taken in the circumferential plane, followed by 350 µm–thick circumferential sections for mechanical testing (n = 2 sections/meniscus). The 350 µm–thick sections were stored in 1× PBS for 24 to 48 hours at 4°C before testing, while the 16 µm–thick sections were used for histological analysis.

Meniscal Histology

Anterior and posterior horn sections (16 µm thick) reserved for histology were fixed in 10% NBF for 10 minutes before safranin-O/fast green staining to

visualize proteoglycan and matrix content.[1,58] Sections were imaged as described earlier, and images were quantified by calculating the percentage area of positive safranin-O staining (open source; ImageJ/FIJI) per cross-sectional area.[6]

Meniscal Tensile Testing

Immediately before tensile testing, circumferential samples were trimmed to a dog-bone shape,[59] and cross-sectional area was measured using a custom, laser-based measurement device.[20] Tensile testing was carried out on an electromechanical testing system (model 5848; Instron), and samples were mounted into serrated grips in a PBS bath to ensure tissue hydration, as described previously.[7] Briefly, samples were preloaded to 0.50 N, underwent 10 cycles of preconditioning (0.5%-2%), and then left to rest for 10 minutes to re-equilibrate. Samples were then tested to failure in tension at a rate of 0.1% strain per second. Toe and linear moduli, as well as the transition point, were calculated through a smooth exponential-linear function fitted to the stress-strain curve,[24,67,77] with the transition point fit via a least squares curve fit. The yield point was defined as the divergence of the stress-strain curve from the linear fit ($r \leq 0.97$).

Synovium Histology and Scoring

Suprapatellar synovium samples were thawed and fixed in 10% NBF for a minimum of 1 day before paraffin processing and embedding. Then, 8 μm–thick sections were cut and stained with hematoxylin-eosin and scored by 3 blinded and trained reviewers (S.B., C.R.S., R.L.M.) for histologic features of synovitis. The following features were scored according to the OARSI guidelines for large-animal models on 5 independent $10\times$ fields from each section: intimal hyperplasia (from 1 to multiple cell layers), inflammatory cell infiltration (from not present to disperse aggregates), subintimal fibrosis (from minimal to dense and widespread), and vascularity (from <3 to >8 vessels per $10\times$ field).[44,69] All sections were stained and scored together. The median score of the 3 reviewers of each subscore for each sample was used for analysis.

Statistical Analysis

Statistical analyses were performed in GraphPad Prism 8 (GraphPad Software). Sham, vertical, and DMM treatment groups were compared using 1-way analysis of variance (ANOVA) when comparing surgical time. For joint contact analysis, meniscal tensile mechanics, cartilage histology scores, and synovium scoring, 2-way ANOVAs were used, with 1 factor being the group and the other being time. Comparisons were made for differences between groups within time points. Treatment group and time point were compared using 2-way ANOVAs when assessing meniscal histology and MRI parameters in the anterior and posterior horns separately. Similarly, microCT, cartilage mechanics, and MRI data were compared using 2-way ANOVAs in the cartilage-cartilage region and cartilage-meniscus regions, separately. Again, comparisons were made for differences

between groups within time points in each location. To verify consistency between scorers, intraclass correlation and percentage agreement measures were calculated after histological scoring. Last, Pearson correlations were performed to identify relationships between outcome measures.

RESULTS

Surgical Details and Postsurgical Recovery

All surgeries were performed without complication, and all animals achieved weightbearing as tolerated within 1 day of surgery, regardless of treatment group. The average surgical time per limb was 40.3 ± 18.7 minutes, with no significant differences between sham, vertical, and DMM limbs ($P > .07$). No animals were removed from the study until their scheduled date of sacrifice (1, 3, or 6 months).

Load Transmission Through the Knee

At 1 month, sham and vertical groups showed similar peak contact pressure and were not different from one another (sham: 1.8 ± 0.4 MPa, vertical: 1.5 ± 0.4 MPa; $P = .87$) while DMM joints had an elevated peak pressure relative to both other groups (3.5 ± 0.9 MPa; $P < .006$) (Figure 2, A and B). Similar results were found in contact area measurements (sham: 152.3 ± 14.7 mm^2, vertical: 152.0 ± 14.9 mm^2; $P = .99$), where DMM joints had significantly decreased contact areas (104.0 ± 29.2 mm^2; $P = .04$) (Figure 2C). These trends disappeared by 3 and 6 months, however, with all groups being statistically similar in terms of peak contact pressure (sham, 3 months: 1.9 ± 0.3 mm^2, vertical, 3 months: 1.9 ± 0.5 mm^2, DMM, 3 months: 2.2 ± 1.1 mm^2 [$P > .55$]; sham, 6 months: 1.7 ± 0.5 mm^2, vertical, 6 months: 1.5 ± 0.4 mm^2, DMM, 6 months: 1.5 ± 0.4 mm^2 [$P > 0.85$]) (Figure 2B) and contact area (sham, 3 months: 144.6 ± 13.3 mm^2, vertical, 3 months: 155.0 ± 20.8 mm^2, DMM, 3 months: 152.2 ± 21.6 mm^2 [$P > .74$]; sham, 6 months: 158.8 ± 25.8 mm^2, vertical, 6 months: 138.0 ± 34.1 mm^2, DMM, 6 months: 141.0 ± 27.3 mm^2 [$P > .42$]) (Figure 2C). This indicates that while DMM caused a marked change in load transfer at 1 month, this resolved by the later time points.

Macroscopic Joint Assessment

Joints were also assessed for macroscopic evidence of injury and wear. Vertical tears were clearly visible in dissected menisci at 3 months (5 of 7 specimens) and 6 months (3 of 4). As described previously,[6] DMM-injured menisci showed a fibrovascular scar at the anterior attachment at 1 month that became more substantial at 3 months. Here, by 6 months, these DMM joints showed continued consolidation of the fibrovascular scar (5 of 5) and substantial narrowing of the anterior cross-sectional width (4 of 5) in the anterior horn (Figure 3A). Very little or no wear was observed in the cartilage of sham-operated joints at all time points. Joints with vertical tears showed minor wear at 1 month (2 of 6), minor (3 of 7) and major (2 of 7) wear at 3 months, and minor wear in all samples (4 of 4) at 6 months.
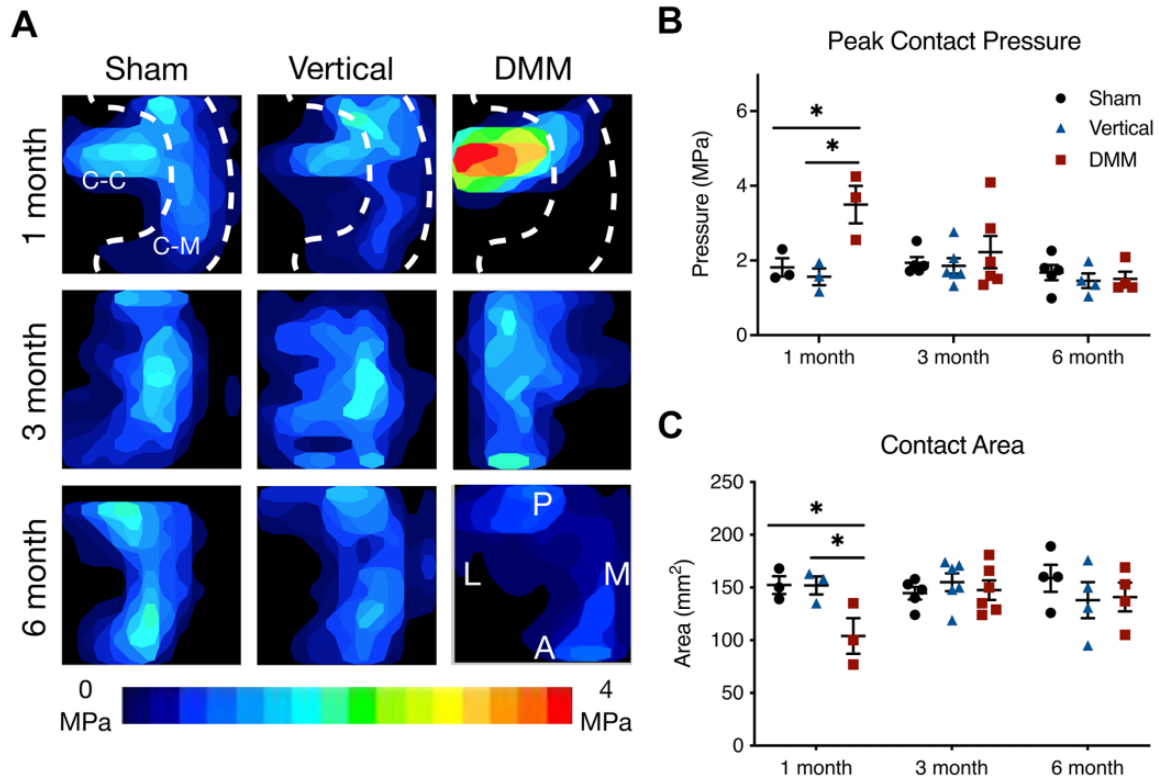
Figure 2. Load transfer in the knee as a function of injury type and time after injury. (A) Representative contact stress maps on the tibial plateau. White-dashed line outlines the approximate location of the meniscus and delineates cartilage-meniscus (C-M) and cartilage-cartilage (C-C) contact areas. (B) Peak contact pressure and (C) contact area calculated from contact maps. A, anterior; DMM, destabilization of the medial meniscus; L, lateral; M, medial; P, posterior. *$P < .05$. Note that data from the sham and DMM groups at the 1- and 3-month time points are reproduced from Bansal et al.[6]

DMM joints showed major cartilage wear that became progressively more apparent at 1 month (2 of 6), 3 months (6 of 7), and 6 months (4 of 5) (Figure 3, B and C). Thus, vertical tears remained visible and caused generally minor cartilage wear, while DMM injuries resulted in the formation and consolidation of an anterior fibrovascular scar, and progressive cartilage wear.

Tibial Plateau Cartilage Mechanical Properties

Cartilage mechanics of the tibial plateau were assessed for each group and at each time point using indentation testing of the region covered by the meniscus (cartilage-meniscus region) and the region not covered by the meniscus (cartilage-cartilage region). In the cartilage-meniscus region, there were no differences between sham and vertical groups at any time point. With DMM, however, there was a decrease in the indentation modulus at 1 month (sham: 1.41 ± 0.27 MPa, DMM: 0.74 ± 0.34 MPa [$P = .002$]; 50% decrease) (Figure 4A). However, by 3 and 6 months, differences between groups were no longer detected. In the cartilage-cartilage region, no differences were detected between sham and vertical groups at any time point. For DMM there was, however, a significant decrease in the indentation modulus at 6 months (sham:

1.61 ± 0.21 MPa, DMM: 1.07 ± 0.22 MPa [$P = .036$]; 33% decrease vs sham) (Figure 4B). These data indicate region-specific and time-dependent changes in tibial plateau cartilage mechanics after DMM injury.

Histological Assessment of Tibial Cartilage and Synovium and microCT Analysis of Subchondral Bone Morphology

Safranin-O/fast green stained sections of the articular cartilage of the tibial plateau were graded using the OARSI scoring system for sheep and goats.[44] Reviewers demonstrated good agreement as determined through intraclass correlation coefficient (95% CI, 0.71-0.86). In general, scores increased (ie, cartilage damage worsened) in the DMM group, with both injury groups resulting in cartilage degeneration by the 6-month time point. Specifically, increased overall scores were observed in vertical injury joints at 6 months (sham, 1 month: 3.2 ± 1.3, vertical, 1 month: 7.3 ± 3.0 [$P = .15$]; sham, 3 months: 2.5 ± 1.8, vertical, 3 months: 3.6 ± 1.6 [$P = .85$]; sham, 6 months: 4.6 ± 1.1, vertical, 6 months: 10.0 ± 2.8 [$P = .073$]), but these did not reach the level of significance. Degeneration in DMM joints started earlier, with significant increases in overall score compared with sham at all time points (DMM, 1 month: 9.0 ± 4.6 [$P = .027$]; DMM, 3 months: 8.2 ± 6.0 [$P = .015$];

DMM, 6 months: 10.4 ± 4.9 [*P* = .036]) (Figure 5, A and B). When examining the subgroups of the OARSI score at the 6-month time point, the "structure" subcategory was the major
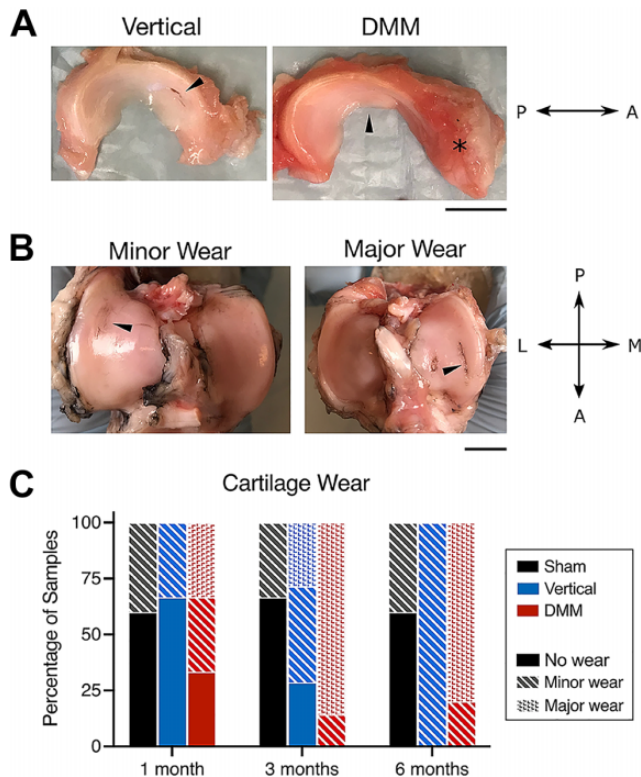

Figure 3. Macroscopic visualization and scoring of joints as a function of injury type and time after injury. (A) Representative images of visible vertical tears (left, arrowhead) and narrowing and scar formation after DMM (right, asterisk). Scale bar = 1 cm. (B) Representative images of minor (left, arrowhead) and major (right, arrowhead) wear on the tibial plateau. Scale bar = 1 cm. (C) Graph showing degree of wear observed for each injury type; no wear (solid bar), minor wear (diagonal fill) and major wear (light fill). A, anterior; DMM, destabilization of the medial meniscus; L, lateral; M, medial; P, posterior.

score-driving component, with differences between sham (0.60 ± 0.55) and both injury groups (vertical: 3.8 ± 2.2 [*P* = .020]; DMM: 4.8 ± 4.3 [*P* = .0002]) (Figure 5C). Despite good agreement between reviewers (range across subscores, percentage agreement within 1 grade: 85%-96%), hematoxylin-eosin staining of synovium showed considerable variability and no significant differences in each subscore at any time point (Figure 6).

MicroCT analysis (BV/TV and trabecular thickness) of the subchondral bone showed no significant differences in either superficial (cartilage-bone interface to 1 mm deep) or deep (2-5 mm deep) zones in both the cartilage-cartilage and cartilage-meniscus contact areas at any time point or with any injury type (Appendix Figures A1 and A2).

Histological Assessment of the Meniscus

Radial sections of the anterior and posterior horn were assessed for proteoglycan content via histology (Figure 7, A and B). Compared with sham, menisci with vertical tears showed decreased proteoglycan content in the anterior horn at 6 months (sham: 0.62 ± 0.08 arbitrary units [a.u.], vertical: 0.44 ± 0.13 a.u. [*P* = .02]), but not before. For DMM-injured menisci, this loss of proteoglycan (Figure 7, A and C) was noted at both 1 and 3 months[6] and persisted through 6 months (DMM anterior horn, 6 months: 0.27 ± 0.08 a.u.; *P* < .0001 vs sham). In the posterior horn, loss of proteoglycan was noted for the DMM group at all time points (sham, 6 months: 0.41 ± 0.07 a.u., DMM, 6 months: 0.26 ± 0.09 a.u. [*P* = .02]), and no changes were seen in this region for vertical injuries (Figure 7, B and D).

Mechanical Assessment of the Meniscus

Bulk tensile testing of the meniscal body region did not detect differences in linear modulus between groups at any time point (*P* = .09). It should be noted, however, that there was large variance in the modulus data at 1 month (sham: 83.0 ± 47.3 MPa, vertical: 79.5 ± 21.9 MPa, DMM: 62.3 ± 29.6 MPa), 3 months (sham: 106.5 ± 50.6 MPa, vertical: 108.2 ± 55.3 MPa, DMM: 71.8 ± 35.0 MPa), and 6 months (sham: 61.6 ± 24.6 MPa, vertical: 65.3 ± 26.5 MPa, DMM: 39.7 ± 10.7 MPa) (Figure 7E). We also did not detect any

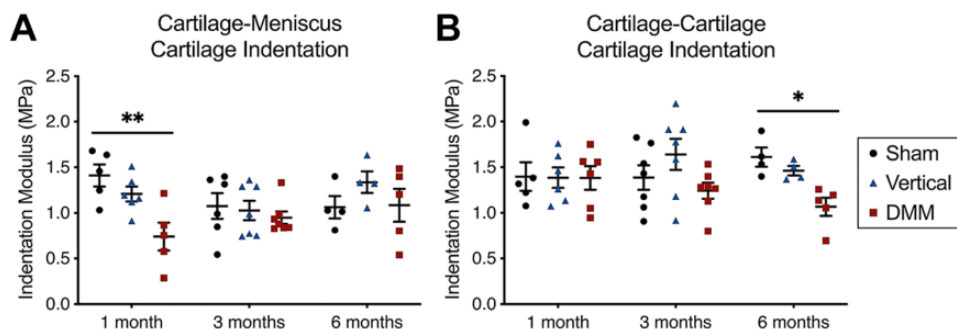**Figure 4.** Mechanical assessment of the tibial plateau articular cartilage as a function of injury type and time after injury. Indentation modulus in the (A) cartilage-meniscus and (B) cartilage-cartilage contact areas. DMM, destabilization of the medial meniscus. **P* < .05, ***P* < .01. Note that data from the sham and DMM groups at the 1- and 3-month time points are reanalyzed from Bansal et al.[6]
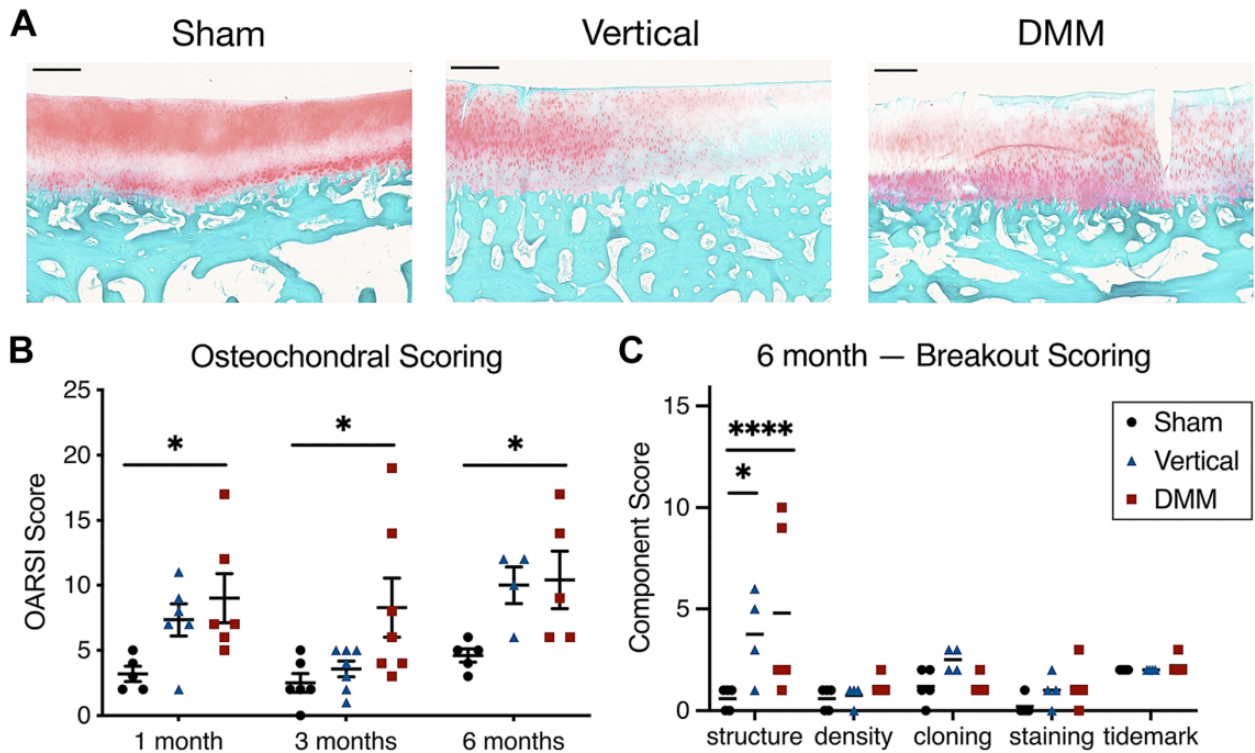
Figure 5. Histological assessment of the tibial plateau articular cartilage as a function of injury type and time after injury. (A) Representative images of osteochondral histology (safranin-O/fast green) of the tibial plateau at 6 months for each group. Scale bar = 500 μ. (B) Aggregate OARSI scoring at each time point and (C) scores from individual categories at 6 months. *P < .05, ****P < .001. Note that samples from the sham and DMM groups at the 1- and 3-month time points are from Bansal et al[6] and here were rescored and reanalyzed by the blinded observers. DMM, destabilization of the medial meniscus; OARSI, Osteoarthritis Research Society International.

changes in toe-region modulus between groups. However, transition strain, the point at which one transitions from the "toe" region to the "linear" region of the stress-strain curve, was affected by meniscal injury. While there were no differences between groups at 1 month (sham: 5.0% ± 2.3%, vertical: 5.0% ± 0.7%, DMM: 5.0% ± 0.4%; $P > .99$) and 3 months (sham: 4.1% ± 0.5%, vertical: 4.1% ± 1.3%, DMM: 4.8% ± 1.3%; $P > .99$), we did note a significant decrease in the transition strain at 6 months in DMM samples (1.6% ± 1.5%) compared with sham (4.3% ± 0.8%; $P = .01$) and vertical (5.4% ± 0.8%; $P = .004$) samples (Figure 7F). These differences were not seen in yield strain.

MRI of the Cartilage and Meniscus

Joints were imaged by MRI at each time point to assess structure and content of the cartilage and meniscus. There were no differences in T_2 values of the cartilage-cartilage region or posterior horn of the meniscus at any time point. As previously reported, DMM joints had T_2 values that were elevated relative to sham in both the cartilage-meniscus region and the anterior horn of the meniscus at the 1-month time point.[6] There were no differences in this measure at either the 3- or 6-month time points. Additionally, there were no differences in T_2 time with vertical tears compared with sham at any time point (Figure 8).

Correlations Between OARSI Score and Meniscal Parameters

Interestingly, cartilage OARSI scores correlated significantly ($P < .05$) with meniscal linear and toe modulus and meniscal safranin-O ratio in the anterior and posterior horns. Given the high level of correlation between linear and toe moduli ($r = 0.77$; $P < 10^{-11}$) and between meniscal safranin-O ratio in both horns ($r = 0.56$; $P < 10^{-5}$), correlations between cartilage OARSI score and meniscal linear modulus and meniscal anterior horn safranin-O ratio were explored. Linear modulus was negatively correlated with OARSI score (Figure 9A) after injury ($r = -0.33$; $P = .019$). Safranin-O ratio of the anterior horn of the meniscus showed an even stronger negative correlation ($r = -0.57$; $P < .0001$) with OARSI score (Figure 9B).

Correlations Between MRI T_2 Times and Mechanical Parameters

Another interesting set of correlations were related to structural T_2 times (via MRI) and mechanical parameters in both the cartilage and the meniscus. Notably, significant correlations were seen between meniscal and cartilage measurements. For example, the T_2 time of the meniscal anterior horn was significantly negatively correlated with
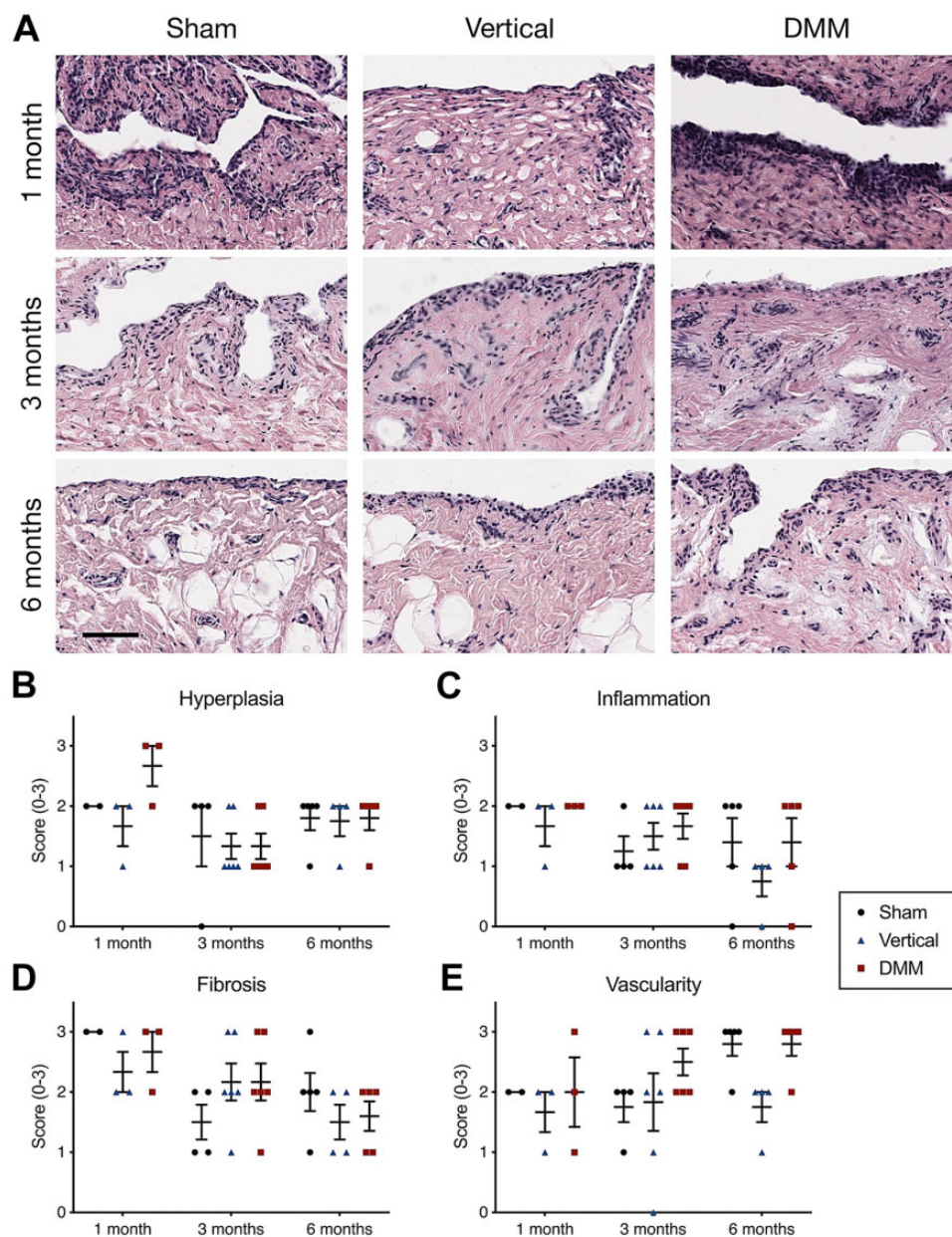
Figure 6. Histological assessment of the synovium as a function of injury type and time after injury. (A) Representative images from each group and time point (hematoxylin-eosin staining). Scale bar = 100 μm. Subscores at each time point for (B) hyperplasia, (C) inflammation, (D) fibrosis, and (E) vascularity. DMM, destabilization of the medial meniscus.

the cartilage indentation modulus in the cartilage-cartilage indentation region (Figure 9C) after injury ($r = -0.35$; $P = .02$). Additionally, the T_2 time of the cartilage-meniscus region showed a significant negative correlation ($r^2 = -0.36$; $P = .02$) with meniscal linear modulus (Figure 9D).

DISCUSSION

In this study, we developed a large-animal model to represent common meniscal injuries and evaluated the consequence of these injuries on overall joint health and

tissue structure and function over a 6-month period. Our findings suggest different trajectories of joint damage as a consequence of these different injury types, which may inform clinical practice regarding appropriateness and timing of intervention.

In general, vertical longitudinal tears resulted in minimal degenerative changes to the joint, despite the persistence of these defects over the 6-month period of study. Notably, the changes that did occur (macroscopic wear, changes in meniscal safranin-O content and osteochondral histopathology) were largely observed at the later 6-month time point (Table 2). This may be owing to the smaller size
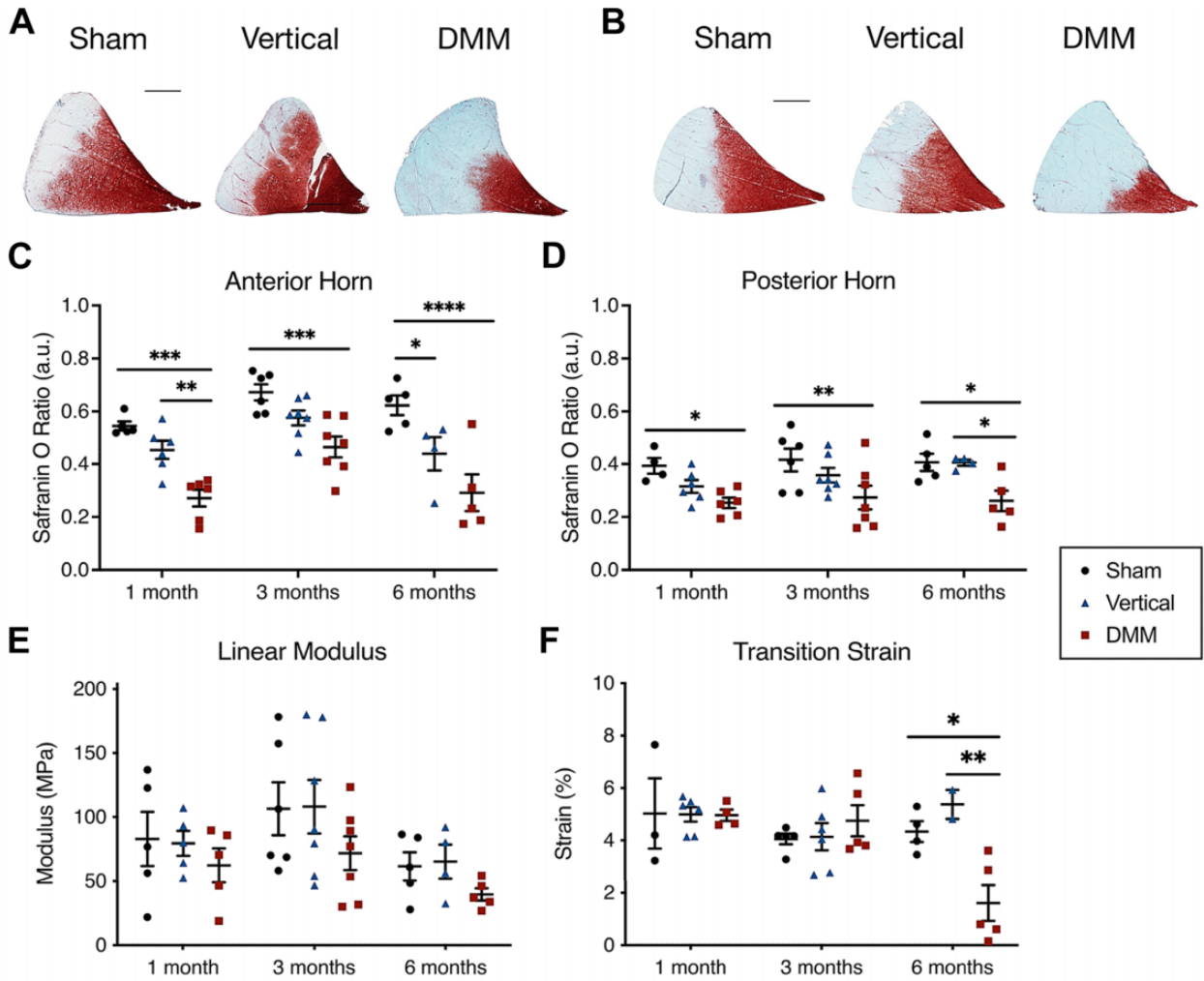
Figure 7. Histological and mechanical assessment of the meniscus as a function of injury type and time after injury. (A) Representative images of anterior horn staining (safranin-O/fast green) at 6 months. Scale bar = 2 mm. (B) Quantification of safranin-O ratio at each time point. Note that data in panels A and B from the sham and DMM groups at the 1- and 3-month time points are reproduced from Bansal et al.[6] (C) Representative images of posterior horn staining (safranin-O/fast green) at 6 months. Scale bar = 2 mm. (D) Quantification of safranin-O ratio at each time point. (E) Linear modulus and (F) transition strain at each time point for samples from each group. *$P < .05$, **$P < .01$, ***$P < .005$, ****$P < .001$. DMM, destabilization of the medial meniscus.

of these injuries, which in clinical practice would not require immediate repair and may have a smaller chance of progression to a more complex bucket-handle tear.[27,80] Indeed, it has been reported that vertical longitudinal tears have a minimal impact on the contact mechanics, whereas bucket-handle tears have a larger impact,[79] suggesting that early-stage vertical longitudinal tears do not immediately create an unstable mechanical environment but have the potential to do so if they grow. The limited changes in overall joint health as a consequence of this type of injury support a nonoperative treatment approach for managing patients with these injuries. This model thus may provide a well-defined test bed for the assessment of novel repair approaches for these types of tears. Indeed, many groups have used a vertical longitudinal tear during ex vivo and large-animal assessment of biologic,[38,74,78,83] scaffold-based,[5,62,65] or surgical

repair[2,4,12,16,48,68] strategies. The stability of this defect and lack of healing observed in the meniscus itself indicate its utility for such studies.

Outcomes of our model of root tears (DMM) are much different than for vertical longitudinal tears, with a mixture of transient, sustained, progressive, and late-arriving degenerative changes across the joint over time. Transient changes include altered joint load transfer, cartilage indentation modulus, MRI T_2 time in the cartilage-meniscus region, and MRI T_2 time in the meniscal anterior horn (Table 2, orange X's). These transient changes are likely the consequence of the formation of the fibrovascular scar at the original insertion site, effectively reestablishing some degree of load transfer at the macroscopic level. However, the presence of sustained and progressive changes such as macroscopic wear of cartilaginous
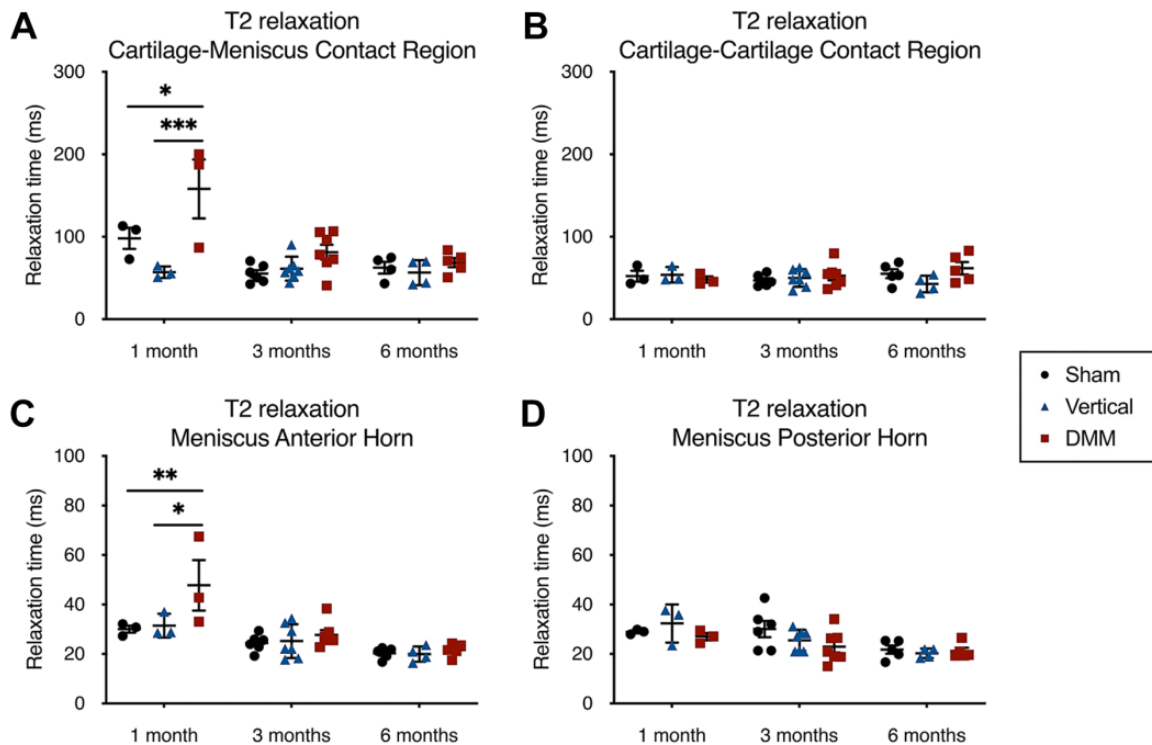
Figure 8. T_2 relaxation times of the (A) cartilage-meniscus and (B) cartilage-cartilage contact regions and (C) meniscal anterior and (D) posterior horn across all groups and time points. *$P < .05$, **$P < .0$, ***$P < .005$. DMM, destabilization of the medial meniscus.

surfaces, narrowing of the meniscus, histopathologic changes to the cartilage surfaces, and loss of proteoglycan in the horns of the meniscus (Table 2, green X's) indicate the continued pathology of the knee joint, even after reestablishment of some load distribution by the meniscus. Those changes that were late-arriving, such as the change in cartilage-cartilage region indentation modulus and change in meniscal transition strain in tension (Table 2, purple X's) underscore the idea that the meniscus and joint continued to remodel well after the detached horn scars down and reattaches. These findings are in agreement with results from open surgical models of anterior horn detachment[55,81] that showed cartilage histopathology at 6 months after injury. These findings are also in agreement with multiple studies utilizing arthroscopic medial meniscal posterior release in a canine model in terms of histopathology,[46] although our findings differ with respect to subchondral bone remodeling (where little was seen in the current study).

It should also be noted that the location of the injuries in this model was in the anterior horn, while injuries (especially root tears) are most common in the posterior horn in humans. The choice of this location was due to the fact that arthroscopic access to the posterior horn was quite challenging, and both anterior and posterior release should have similar impacts on the meniscus itself, abrogating its ability to generate hoop stresses, regardless of location. Our observations in this DMM response are reminiscent of the clinical finding that nonanatomic repair after root tears has an adverse impact on healing[41,72] and that a reattachment

that does not reapproximate the anatomic enthesis does not protect the meniscus and joint. Therefore, in our model, it is likely that the meniscal attachment "healed" and reattached such that it afforded some degree of effective joint-level load bearing but did not achieve tissue-level homeostasis. Clinically, it has been reported that distance between the meniscus horn and its insertion in root tears is positively correlated with worse outcomes.[33] This may account for the milder response we observed in this model compared with other models in which a large segmental removal of the anterior horn leads to much worse outcomes at this time point.[81] Regardless, our data indicate that, absent appropriate fixation of a root tear, the joint will progressively deteriorate, in a similar manner to the murine DMM models on which it was based. This also provides a new surgical model to test the timing and efficacy of such repair procedures on long-term joint health and may direct clinical practice.

Other interesting findings are the correlations relating histopathologic changes in cartilage (a hallmark of OA) and meniscal properties. Joint degeneration is just that, a joint-wide phenomenon, and our findings suggest that, in response to an unloading meniscal injury, meniscus extracellular matrix (glycosaminoglycan content) and meniscal functional properties (linear modulus) are indicators of worsening outcomes across the joint. To our knowledge, this is the first study to show the extent of meniscal degeneration in concert with cartilage wear and degeneration. Additionally, correlations of T_2 time to meniscal and cartilage function underscore the utility of MRI as a predictive,
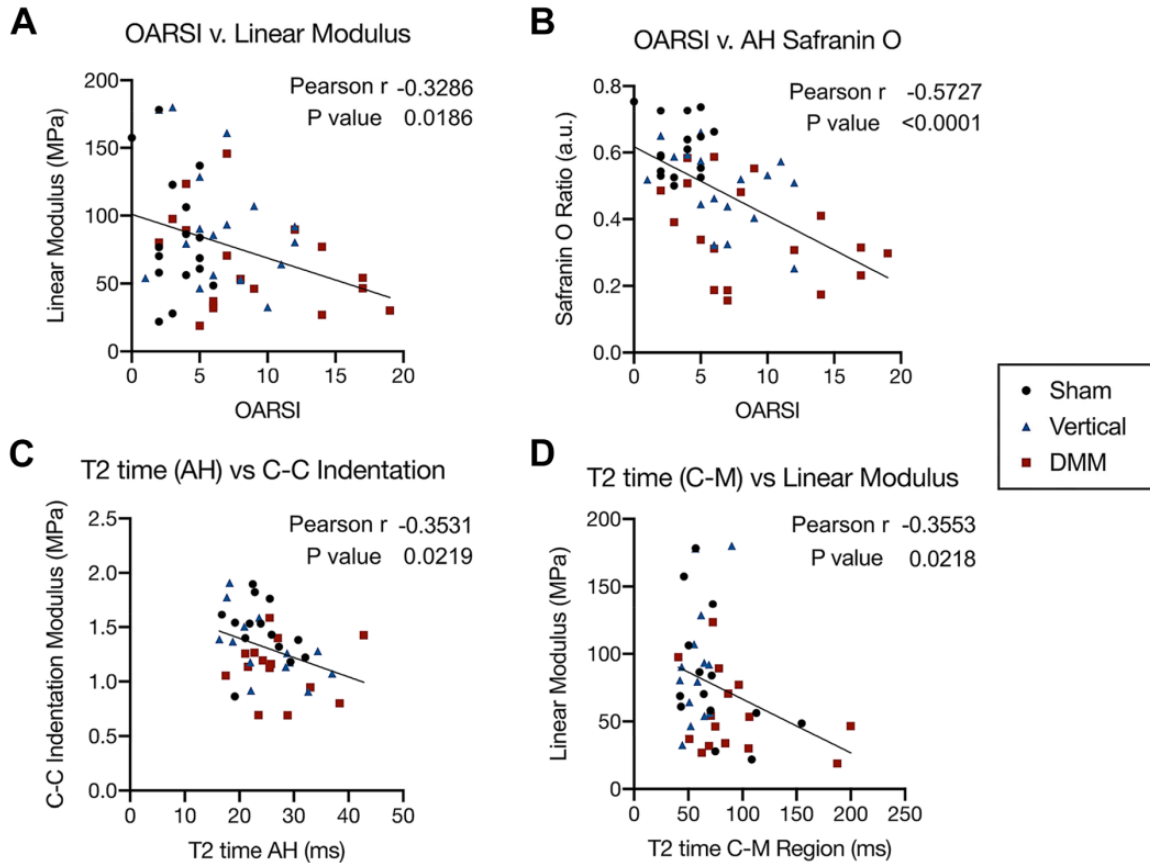
Figure 9. Correlations of Osteoarthritis Research Society International (OARSI) scores with (A) meniscal tensile linear modulus and (B) meniscal safranin-O ratio in the anterior horn (AH). Correlations of (C) T_2 times of the meniscal AH with cartilage-cartilage (C-C) indentation modulus and (D) T_2 times of the cartilage-meniscus (C-M) region with meniscal linear modulus. DMM, destabilization of the medial meniscus.

TABLE 2
Summary Table Showing Changes to the Joint Space, Cartilage and Bone, and Meniscus[a]

| | | Vertical Longitudinal Tear | DMM | | | Change |
			1 mo	3 mo	6 mo	
Joint	Joint load transfer	–	↓	–	–	X
	Macroscopic assessment	Visible	↓	↓↓	↓↓↓	X
	Synovitis	–	–	–	–	
Cartilage/Bone	Indentation modulus (C-M)	–	↓	–	–	X
	Indentation modulus (C-C)	–	–	–	↓	X
	MicroCT	–	–	–	–	
	MRI T2 time	–	↑ (C-M)	–	–	X
	OARSI score	↑ (6 mo)	↑	↑	↑	X
Meniscus	Tensile bulk mechanics	–	–	–	↓ (txn)	X
	MRI T2 time	–	↑ (AH)	–	–	X
	Safranin-O staining (AH)	↓ (6 mo)	↓	↓	↓↓	X
	Safranin-O staining (PH)	–	↓	↓	↓	X

[a]Vertical longitudinal tear time points are combined, whereas DMM time points are split. The number of arrows indicates the severity of the change. Dashes indicate no significant change compared to Sham. Orange X's denote transient changes, green X's denote sustained changes, and purple X's denote late-arriving changes after injury. AH, anterior horn; C-C, cartilage-cartilage; C-M, cartilage-meniscus; DMM, destabilization of the medial meniscus; MicroCT, micro–computed tomography; MRI, magnetic resonance imaging; OARSI, Osteoarthritis Research Society International; PH, posterior horn; txn, transition strain.

noninvasive, and longitudinal measure to follow and predict both cartilage and meniscal degeneration.

This model has some limitations. In accordance with Institutional Animal Care and Use Committee guidelines to reduce animal numbers, we utilized a bilateral model instead of unilateral surgeries with nonoperative contralateral controls. The possible effects of contralateral treatment are undetermined. Bilateral model notwithstanding, the sample size remained low, leading to some variability in outcome measures. This variability is most notable in meniscal tensile mechanics, which has high donor-to-donor and sample-to-sample variability for both porcine[40] and human[23] donor tissue. There is additional variability when assessing histopathology, particularly in injury groups at the longest, 6-month time point. This suggests that some experimental subjects continued to experience progressive cartilage degeneration with time, whereas others stabilized after injury. Longer time points would likely clarify progression of this injury response. Additionally, this study utilized juvenile animals (age 6 months), as they are more likely to have a healthy knee at time zero and because juvenile porcine menisci can remodel in response to changes in loading conditions, that is, with development and sustained load.[7,29,30,43,61] However, juvenile animals mature, and some of the temporal changes seen in this study may be due to development and not intervention. While the goal of this study was primarily to understand the etiology of meniscal degeneration secondary to injury, repeating these studies in larger, skeletally mature animals may provide further insight and clinical relevance. Last, microscale assays investigating catabolic extracellular matrix digestion may provide additional spatiotemporal understanding of the progression of degeneration.

CONCLUSION

This porcine model detailed the whole-joint impacts of 2 types of clinically relevant meniscal tears. This model indicates a slower and milder progression than other, more aggressive studies, and therefore may better mimic those acute but smaller clinical tears that progress to joint deterioration. Our finding that small vertical longitudinal tears cause minor pathological changes to the joint that took 6 months to be apparent reaffirms the relevance of tear size and orientation in clinical management of meniscal tears. Additionally, the spontaneous reattachment of the anterior meniscal attachment after DMM, while likely not physiologically relevant in the posterior horn of human patients, indicates the importance of root reattachments. In particular, these data suggest that in the absence of a timely and mechanically competent fixation method, the joint may not recover from a root tear. Last, the correlations between meniscal degeneration and cartilage histopathology indicate that in the context of meniscal injury, OA is an interconnected disease of both the cartilage and the meniscus. Now that it has been established, this model may serve as a test bed for experimental surgical, scaffold-based, and small molecule-driven interventions after injury to prevent OA development and will support further studies on

meniscal repair. This model also supports the field of sports medicine by detailing the early progression of degeneration after clinically relevant meniscal tears.

ACKNOWLEDGMENT

REFERENCES

1. Andrews SHJ, Rattner JB, Jamniczky HA, Shrive NG, Adesida AB. The structural and compositional transition of the meniscal roots into the fibrocartilage of the menisci. *J Anat*. 2015;226(2):169-174. doi:10.1111/joa.12265
2. Arnoczky SP, Lavagnino M. Tensile fixation strengths of absorbable meniscal repair devices as a function of hydrolysis time: an in vitro experimental study. *Am J Sports Med*. 2001;29(2):118-123. doi:10.1177/03635465010290020201
3. Arnoczky SP, Warren RF. Microvasculature of the human meniscus. *Am J Sports Med*. 1982;10(2):90-95. doi:10.1177/036354658201000205
4. Aros BC, Pedroza A, Vasileff WK, Litsky AS, Flanigan DC. Mechanical comparison of meniscal repair devices with mattress suture devices in vitro. *Knee Surg Sports Traumatol Arthrosc*. 2010;18(11):1594-1598. doi:10.1007/s00167-010-1188-z
5. Baek J, Lotz MK, D'lima DD. Core-shell nanofibrous scaffolds for repair of meniscus tears. *Tissue Eng - Part A*. 2019;25(23-24):1577-1590. doi:10.1089/ten.tea.2018.0319
6. Bansal S, Miller LM, Patel JM, et al. Transection of the medial meniscus anterior horn results in cartilage degeneration and meniscus remodeling in a large animal model. *J Orthop Res*. 2020;38(12):2696-2708.
7. Bansal S, Peloquin JM, Keah NM, et al. Structure, function, and defect tolerance with maturation of the radial tie fiber network in the knee meniscus. *J Orthop Res*. 2020;38(12):2709-2720.
8. Beamer BS, Walley KC, Okajima S, et al. Changes in contact area in meniscus horizontal cleavage tears subjected to repair and resection. *Arthroscopy*. 2017;33(3):617-624. doi:10.1016/j.arthro.2016.09.004
9. Bedi A, Kelly NH, Baad M, et al. Dynamic contact mechanics of the medial meniscus as a function of radial tear, repair, and partial meniscectomy. *J Bone Joint Surg Am*. 2010;92(6):1398-1408. doi:10.2106/JBJS.I.00539
10. Bhatia S, LaPrade CM, Ellman MB, LaPrade RF. Meniscal root tears: significance, diagnosis, and treatment. *Am J Sports Med*. 2014;42(12):3016-3030. doi:10.1177/0363546514524162
11. Chahla J. Editorial commentary: meniscal root repairs: let the biology help you! *Arthroscopy*. 2019;35(4):1240-1242. doi:10.1016/j.arthro.2018.12.026
12. Chang HC, Nyland J, Caborn DNM, Burden R. Biomechanical evaluation of meniscal repair systems: a comparison of the meniscal viper repair system, the vertical mattress FasT-Fix device, and vertical mattress ethibond sutures. *Am J Sports Med*. 2005;33(12):1846-1852. doi:10.1177/0363546505278254
13. Chen Z, Zhang H, Luo H, et al. Contact mechanics after mattress suture repair of medial meniscus vertical longitudinal tear: an in vitro study. *Arch Orthop Trauma Surg*. 2020;140:1221-1230. doi:10.1007/s00402-020-03428-0

14. Chery DR, Han B, Li Q, et al. Early changes in cartilage pericellular matrix micromechanobiology portend the onset of post-traumatic osteoarthritis. *Acta Biomater*. 2020;111:267-278. doi:10.1016/j.actbio.2020.05.005

15. Chhabra A, Ashikyan O, Hlis R, et al. The International Society of Arthroscopy, Knee Surgery and Orthopaedic Sports Medicine classification of knee meniscus tears: three-dimensional MRI and arthroscopy correlation. *Eur Radiol*. 2019;29(11):6372-6384. doi:10.1007/s00330-019-06220-w

16. Cook JL, Fox DB. A novel bioabsorbable conduit augments healing of avascular meniscal tears in a dog model. *Am J Sports Med*. 2007;35(11):1877-1887. doi:10.1177/0363546507304330

17. Doral MN, Bilge O, Huri G, Turhan E, Verdonk R. Modern treatment of meniscal tears. *EFORT Open Rev*. 2018;3(5):260-268. doi:10.1302/2058-5241.3.170067

18. Doyran B, Tong W, Li Q, et al. Nanoindentation modulus of murine cartilage: a sensitive indicator of the initiation and progression of post-traumatic osteoarthritis. *Osteoarthritis Cartilage*. 2017;25(1):108-117. doi:10.1016/j.joca.2016.08.008

19. Englund M, Roos EM, Lohmander LS. Impact of type of meniscal tear on radiographic and symptomatic knee osteoarthritis: a sixteen-year followup of meniscectomy with matched controls. *Arthritis Rheum*. 2003;48(8):2178-2187. doi:10.1002/art.11088

20. Favata M. *Scarless Healing in the Fetus: Implications and Strategies for Postnatal Tendon Repair*. Published online 2006. http://repository.upenn.edu/dissertations/AAI3246156/

21. Fisher MB, Belkin NS, Milby AH, et al. Cartilage repair and subchondral bone remodeling in response to focal lesions in a mini-pig model: implications for tissue engineering. *Tissue Eng Part A*. 2015;21(3-4):850-860. doi:10.1089/ten.tea.2014.0384

22. Fisher MB, Belkin NS, Milby AH, et al. Effects of mesenchymal stem cell and growth factor delivery on cartilage repair in a mini-pig model. *Cartilage*. 2016;7(2):174-184. doi:10.1177/1947603515623030

23. Fithian DC, Kelly MA, Mow VC. Material properties and structure-function relationships in the menisci. *Clin Orthop Relat Res*. 1990;252:19-31. http://www.ncbi.nlm.nih.gov/pubmed/2406069

24. Fung YCB. Elasticity of soft tissues in simple elongation. *Am J Physiol*. 1967;213(6):1532-1544.

25. Ghodbane SA, Patel JM, Brzezinski A, Lu TM, Gatt CJ, Dunn MG. Biomechanical characterization of a novel collagen-hyaluronan infused 3D-printed polymeric device for partial meniscus replacement. *J Biomed Mater Res B Appl Biomater*. 2019;107(8):2457-2465. doi:10.1002/jbm.b.34336

26. Glasson SS, Blanchet TJ, Morris EA. The surgical destabilization of the medial meniscus (DMM) model of osteoarthritis in the 129/SvEv mouse. *Osteoarthritis Cartilage*. 2007;15(9):1061-1069. doi:10.1016/j.joca.2007.03.006

27. Goyal KS, Pan TJ, Tran D, Dumpe SC, Zhang X, Harner CD. Vertical tears of the lateral meniscus: effects on in vitro tibiofemoral joint mechanics. *Orthop J Sports Med*. 2014;2(8):2325967114541237.

28. Haase T, Sunkara V, Kohl B, et al. Discerning the spatio-temporal disease patterns of surgically induced OA mouse models. *PLoS One*. 2019;14(4):e0213734. doi:10.1371/journal.pone.0213734

29. Han WM, Heo S-J, Driscoll TP, et al. Microstructural heterogeneity directs micromechanics and mechanobiology in native and engineered fibrocartilage. *Nat Mater*. 2016;15(4):477-484. doi:10.1038/nmat4520

30. Ionescu LC, Lee GC, Sennett BJ, Burdick JA, Mauck RL. An anisotropic nanofiber/microsphere composite with controlled release of biomolecules for fibrous tissue engineering. *Biomaterials*. 2010;31(14):4113-4120. doi:10.1016/j.biomaterials.2010.01.098

31. Jones RS, Keene GCR, Learmonth DJA, et al. Direct measurement of hoop strains in the intact and torn human medial meniscus. *Clin Biomech (Bristol, Avon)*. 1996;11(5):295-300. doi:10.1016/0268-0033(96)00003-4

32. Jung YH, Choi NH, Oh JS, Victoroff BN. All-inside repair for a root tear of the medial meniscus using a suture anchor. *Am J Sports Med*. 2012;40(6):1406-1411. doi:10.1177/0363546512439181

33. Kim JY, Bin S-I, Kim JM, Lee BS, Oh SM, Cho WJ. A novel arthroscopic classification of degenerative medial meniscus posterior root tears based on the tear gap. *Orthop J Sports Med*. 2019;7(3):2325967119827945. doi:10.1177/2325967119827945

34. Koo JH, Choi SH, Lee SA, Wang JH. Comparison of medial and lateral meniscus root tears. *PLoS One*. 2015;10(10):e0141021. doi:10.1371/journal.pone.0141021

35. Kopf S, Beaufils P, Hirschmann MT, et al. Management of traumatic meniscus tears: the 2019 ESSKA meniscus consensus. *Knee Surg Sports Traumatol Arthrosc*. 2020;28(4):1177-1194. doi:10.1007/s00167-020-05847-3

36. Krych AJ, Johnson NR, Mohan R, Dahm DL, Levy BA, Stuart MJ. Partial meniscectomy provides no benefit for symptomatic degenerative medial meniscus posterior root tears. *Knee Surg Sports Traumatol Arthrosc*. 2018;26(4):1117-1122. doi:10.1007/s00167-017-4454-5

37. Krych AJ, Reardon PJ, Johnson NR, et al. Non-operative management of medial meniscus posterior horn root tears is associated with worsening arthritis and poor clinical outcome at 5-year follow-up. *Knee Surg Sports Traumatol Arthrosc*. 2017;25(2):383-389. doi:10.1007/s00167-016-4359-8

38. Kurnaz R, Balta O. Effect of platelet-rich plasma and platelet-rich fibrin matrix on healing of vertical meniscal tears in a rabbit model. *Acta Orthop Traumatol Turc*. 2020;54(2):186-195. doi:10.5152/j.aott.2020.02.20

39. Kuroki K, Cook CR, Cook JL. Subchondral bone changes in three different canine models of osteoarthritis. *Osteoarthritis Cartilage*. 2011;19(9):1142-1149. doi:10.1016/j.joca.2011.06.007

40. Lakes EH, Kline CL, McFetridge PS, Allen KD. Comparing the mechanical properties of the porcine knee meniscus when hydrated in saline versus synovial fluid. *J Biomech*. 2015;48(16):4333-4338. doi:10.1016/j.jbiomech.2015.10.046

41. LaPrade CM, Foad A, Smith SD, et al. Biomechanical consequences of a nonanatomic posterior medial meniscal root repair. *Am J Sports Med*. 2015;43(4):912-920. doi:10.1177/0363546514566191

42. LaPrade RF, Moulton SG, Cram TR, Geeslin AG, LaPrade CM, Engebretsen L. Meniscal root repairs. *JBJS Essent Surg Tech*. 2015;5(4):e19. doi:10.2106/JBJS.ST.N.00098

43. Li Q, Wang C, Han B, et al. Impacts of maturation on the micromechanics of the meniscus extracellular matrix. *J Biomech*. 2018;72:252-257. doi:10.1016/j.jbiomech.2018.02.037

44. Little CB, Smith MM, Cake MA, Read RA, Murphy MJ, Barry FP. The OARSI histopathology initiative – recommendations for histological assessments of osteoarthritis in sheep and goats. *Osteoarthritis Cartilage*. 2010;18(suppl_3):S80-S92. doi:10.1016/j.joca.2010.04.016

45. Loeser RF, Olex AL, McNulty MA, et al. Disease progression and phasic changes in gene expression in a mouse model of osteoarthritis. *PLoS One*. 2013;8(1):e54633. doi:10.1371/journal.pone.0054633

46. Luther JK, Cook CR, Cook JL. Meniscal release in cruciate ligament intact stifles causes lameness and medial compartment cartilage pathology in dogs 12 weeks postoperatively. *Vet Surg*. 2009;38(4):520-529. doi:10.1111/j.1532-950X.2009.00520.x

47. Meloni GR, Fisher MB, Stoeckl BD, Dodge GR, Mauck RL. Biphasic finite element modeling reconciles mechanical properties of tissue-engineered cartilage constructs across testing platforms. *Tissue Eng - Part A*. 2017;23(13-14):663-674. doi:10.1089/ten.tea.2016.0191

48. Milchteim C, Branch EA, Maughon T, Hughey J, Anz AW. Biomechanical comparison of parallel and crossed suture repair for longitudinal meniscus tears. *Orthop J Sports Med*. 2016;4(4):2325967116640263. doi:10.1177/2325967116640263

49. Miller RE, Belmadani A, Ishihara S, et al. Damage-associated molecular patterns generated in osteoarthritis directly excite murine nociceptive neurons through toll-like receptor 4. *Arthritis Rheumatol*. 2015;67(11):2933-2943. doi:10.1002/art.39291

50. Mononen ME, Jurvelin JS, Korhonen RK. Effects of radial tears and partial meniscectomy of lateral meniscus on the knee joint mechanics during the stance phase of the gait cycle—a 3D finite element study. *J Orthop Res*. 2013;31(8):1208-1217. doi:10.1002/jor.22358

51. Mordecai SC. Treatment of meniscal tears: an evidence based approach. *World J Orthop*. 2014;5(3):233. doi:10.5312/wjo.v5.i3.233

52. Mosher TJ, Dardzinski BJ, Smith MB. Human articular cartilage: influence of aging and early symptomatic degeneration on the spatial variation of T2—preliminary findings at 3 T. *Radiology*. 2000;214(1):259-266. doi:10.1148/radiology.214.1.r00ja15259

53. Nebelung S, Tingart M, Pufe T, Kuhl C, Jahr H, Truhn D. Ex vivo quantitative multiparametric MRI mapping of human meniscus degeneration. *Skeletal Radiol*. 2016;45(12):1649-1660. doi:10.1007/s00256-016-2480-x

54. Nishida M, Higuchi H, Kobayashi Y, Takagishi K. Histological and biochemical changes of experimental meniscus tear in the dog knee. *J Orthop Sci*. 2005;10(4):406-413. doi:10.1007/s00776-005-0916-6

55. Oláh T, Reinhard J, Gao L, et al. Topographic modeling of early human osteoarthritis in sheep. *Sci Transl Med*. 2019;11(508):eAAX6775. doi:10.1126/scitranslmed.aax6775

56. Padalecki JR, Jansson KS, Smith SD, et al. Biomechanical consequences of a complete radial tear adjacent to the medial meniscus posterior root attachment site: in situ pull-out repair restores derangement of joint mechanics. *Am J Sports Med*. 2014;42(3):699-707. doi:10.1177/0363546513499314

57. Pashuck TD, Kuroki K, Cook CR, Stoker AM, Cook JL. Hyaluronic acid versus saline intra-articular injections for amelioration of chronic knee osteoarthritis: a canine model. *J Orthop Res*. 2016;34(10):1772-1779. doi:10.1002/jor.23191

58. Pauli C, Grogan SP, Patil S, et al. Macroscopic and histopathologic analysis of human knee menisci in aging and osteoarthritis. *Osteoarthritis Cartilage*. 2011;19(9):1132-1141. doi:10.1016/j.joca.2011.05.008

59. Peloquin JM, Elliott DM. A comparison of stress in cracked fibrous tissue specimens with varied crack location, loading, and orientation using finite element analysis. *J Mech Behav Biomed Mater*. 2016;57:260-268. doi:10.1016/j.jmbbm.2015.12.004

60. Pfeifer CG, Fisher MB, Saxena V, et al. Age-dependent subchondral bone remodeling and cartilage repair in a minipig defect model. *Tissue Eng - Part C Methods*. 2017;23(11):745-753. doi:10.1089/ten.tec.2017.0109

61. Qu F, Li Q, Wang X, et al. Maturation state and matrix microstructure regulate interstitial cell migration in dense connective tissues. *Sci Rep*. 2018;8(1):3295. doi:10.1038/s41598-018-21212-4

62. Qu F, Pintauro MP, Haughan JE, et al. Repair of dense connective tissues via biomaterial-mediated matrix reprogramming of the wound interface. *Biomaterials*. 2015;39:85-94. doi:10.1016/j.biomaterials.2014.10.067

63. Qu F, Stoeckl BD, Gebhard PM, Hullfish TJ, Baxter JR, Mauck RL. A wearable magnet-based system to assess activity and joint flexion in humans and large animals. *Ann Biomed Eng*. 2018;46(12):2069-2078. doi:10.1007/s10439-018-2105-8

64. Rauscher I, Stahl R, Cheng J, et al. Meniscal measurements of T1ρ and T2 at MR imaging in healthy subjects and patients with osteoarthritis. *Radiology*. 2008;249(2):591-600. doi:10.1148/radiol.2492071870

65. Resmi R, Parvathy J, John A, Joseph R. Injectable self-crosslinking hydrogels for meniscal repair: a study with oxidized alginate and gelatin. *Carbohydr Polym*. 2020;234:115902.

66. Roos H, Adalberth T, Dahlberg L, Lohmander LS. Osteoarthritis of the knee after injury to the anterior cruciate ligament or meniscus: the influence of time and age. *Osteoarthritis Cartilage*. 1995;3(4):261-267.

67. Roth V, Mow VC. The intrinsic tensile behaviour of the matrix of bovine articular cartilage and its variations with age. *J Bone Joint Surg*. 1980;62(7):1102-1117.

68. Sandmann GH, Adamczyk C, Garcia EG, et al. Biomechanical comparison of menisci from different species and artificial constructs. *BMC Musculoskelet Disord*. 2013;14(1):324. doi:10.1186/1471-2474-14-324

69. Scanzello CR, Albert AS, DiCarlo E, et al. The influence of synovial inflammation and hyperplasia on symptomatic outcomes up to 2 years post-operatively in patients undergoing partial meniscectomy. *Osteoarthritis Cartilage*. 2013;21(9):1392-1399. doi:10.1016/j.joca.2013.05.011

70. Seo J-H, Li G, Shetty GM, et al. Effect of repair of radial tears at the root of the posterior horn of the medial meniscus with the pullout suture technique: a biomechanical study using porcine knees. *Arthroscopy*. 2009;25(11):1281-1287. doi:10.1016/j.arthro.2009.05.014

71. Son M, Goodman SB, Chen W, Hargreaves BA, Gold GE, Levenston ME. Regional variation in T1ρ and T2 times in osteoarthritic human menisci: correlation with mechanical properties and matrix composition. *Osteoarthritis Cartilage*. 2013;21(6):796-805. doi:10.1016/j.joca.2013.03.002

72. Stärke C, Kopf S, Gröbel K-H, Becker R. The effect of a nonanatomic repair of the meniscal horn attachment on meniscal tension: a biomechanical study. *Arthroscopy*. 2010;26(3):358-365. doi:10.1016/j.arthro.2009.08.013

73. Steineman BD, LaPrade RF, Haut Donahue TL. Loosening of transtibial pullout meniscal root repairs due to simulated rehabilitation is unrecoverable: a biomechanical study. *Arthroscopy*. 2019;35(4):1232-1239. doi:10.1016/j.arthro.2018.11.041

74. Steinert AF, Palmer GD, Capito R, et al. Genetically enhanced engineering of meniscus tissue using ex vivo delivery of transforming growth factor-beta 1 complementary deoxyribonucleic acid. *Tissue Eng*. 2007;13(9):2227-2237. doi:10.1089/ten.2006.0270

75. Tachibana Y, Mae T, Fujie H, et al. Effect of radial meniscal tear on in situ forces of meniscus and tibiofemoral relationship. *Knee Surg Sports Traumatol Arthrosc*. 2017;25(2):355-361. doi:10.1007/s00167-016-4395-4

76. Takao S, Nguyen TB, Yu HJ, et al. T1rho and T2 relaxation times of the normal adult knee meniscus at 3 T: analysis of zonal differences. *BMC Musculoskelet Disord*. 2017;18(1):1-9. doi:10.1186/s12891-017-1560-y

77. Tanaka ML, Weisenbach CA, Carl Miller M, Kuxhaus L. A continuous method to compute model parameters for soft biological materials. *J Biomech Eng*. 2011;133(7):074502. doi:10.1115/1.4004412

78. Tarafder S, Gulko J, Sim KH, Yang J, Cook JL, Lee CH. Engineered healing of avascular meniscus tears by stem cell recruitment. *Sci Rep*. 2018;8(1):1-9. doi:10.1038/s41598-018-26545-8

79. Thieman KM, Pozzi A, Ling HY, Lewis DD, Horodyski M. Contact mechanics of simulated meniscal tears in cadaveric canine stifles. *Vet Surg*. 2009;38(7):803-810. doi:10.1111/j.1532-950X.2009.00571.x

80. Vaquero-Picado A, Rodríguez-Merchán EC. Arthroscopic repair of the meniscus: surgical management and clinical outcomes. *EFORT Open Rev*. 2018;3(11):584-594. doi:10.1302/2058-5241.3.170059

81. Waller KA, Chin KE, Jay GD, et al. Intra-articular recombinant human proteoglycan 4 mitigates cartilage damage after destabilization of the medial meniscus in the Yucatan minipig. *Am J Sports Med*. 2017;45(7):1512-1521. doi:10.1177/0363546516686965

82. Zdero R. *Experimental Methods in Orthopaedic Biomechanics*. Elsevier; 2017. doi:10.1016/C2015-0-00572-X

83. Zhang H, Leng P, Zhang J. Enhanced meniscal repair by overexpression of hIGF-1 in a full-thickness model. *Clin Orthop Relat Res*. 2009;467(12):3165-3174. doi:10.1007/s11999-009-0921-8

84. Zhang K, Li L, Yang L, et al. The biomechanical changes of load distribution with longitudinal tears of meniscal horns on knee joint: a finite element analysis. *J Orthop Surg Res*. 2019;14(1):237. doi:10.1186/s13018-019-1255-1
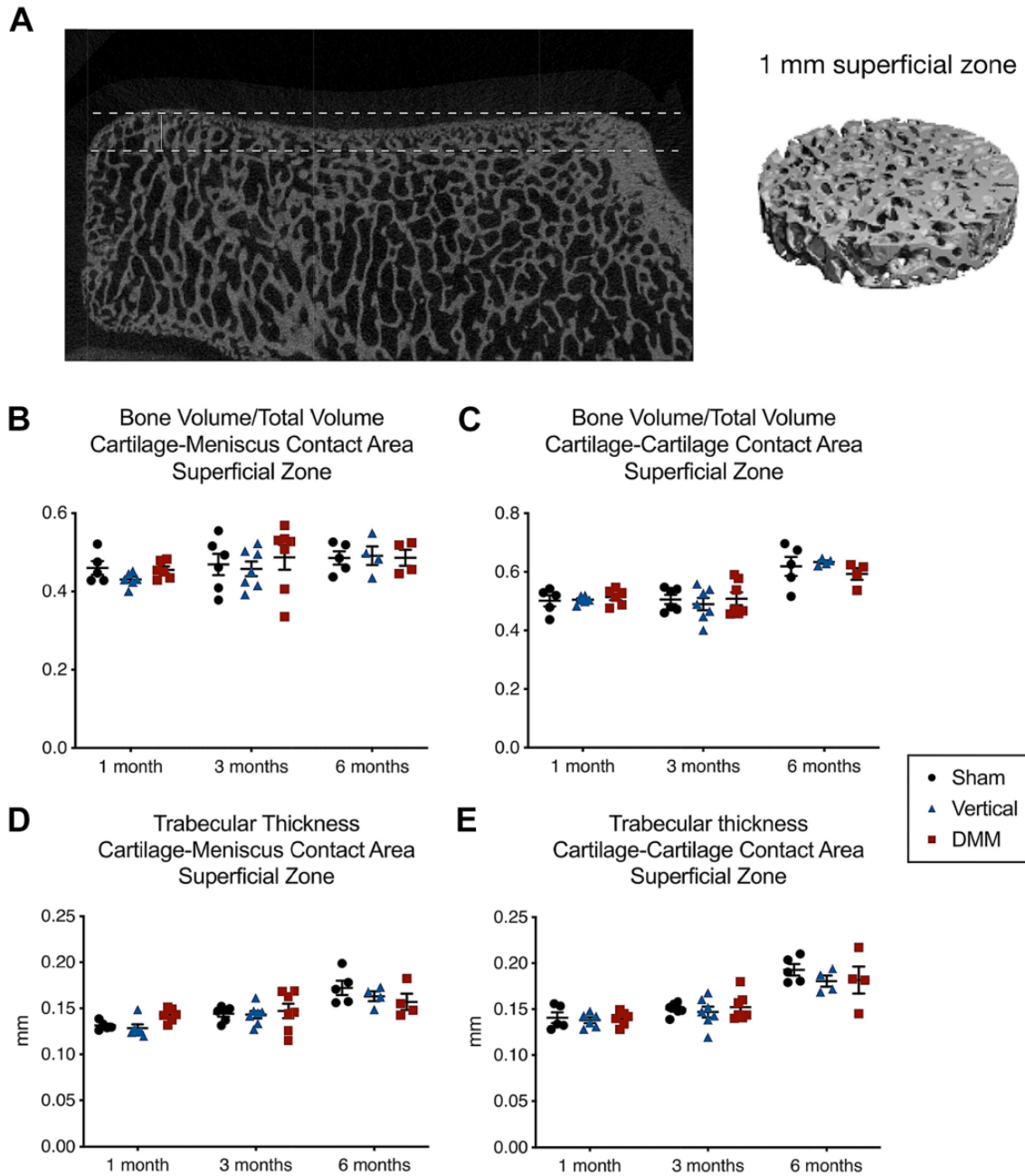
APPENDIX

Figure A1. (A) Micro–computed tomography analysis of the superficial zone, a zone 1 mm deep from the surface. Bone volume/ total volume in the (B) cartilage-meniscus contact area and (C) cartilage-cartilage contact areas. Trabecular thickness in the (D) cartilage-meniscus contact area and (E) cartilage-cartilage contact areas. DMM, destabilization of the medial meniscus.
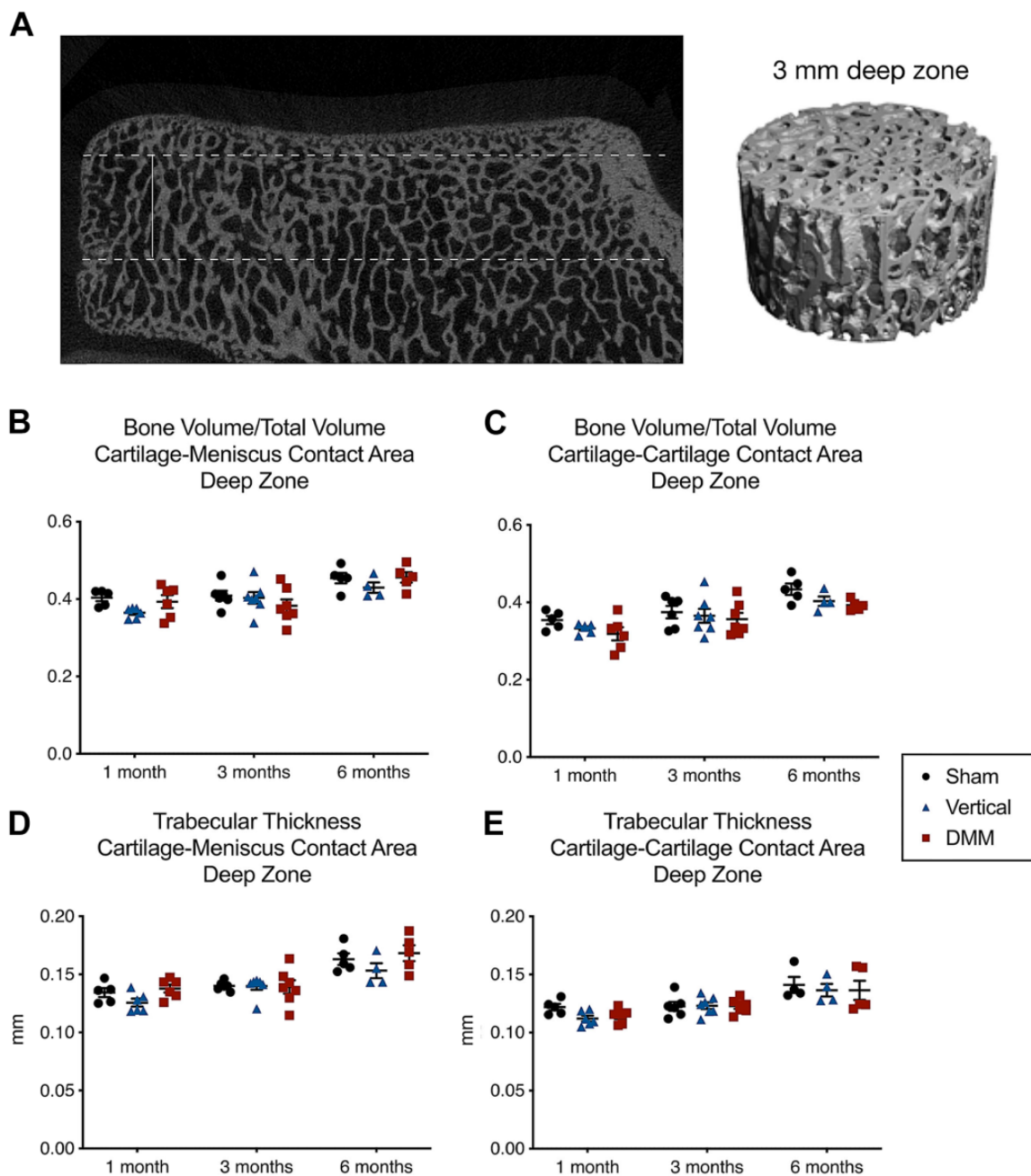
Figure A2. (A) Micro–computed tomography analysis of the deep zone, a zone 2 mm deep from the surface and extending another 3 mm deep from there. Bone volume/total volume in the (B) cartilage-meniscus contact area and (C) cartilage-cartilage contact areas. Trabecular thickness in the (D) cartilage-meniscus contact area and (E) cartilage-cartilage contact areas. DMM, destabilization of the medial meniscus.